Dossier

This paper is a part of the hereunder thematic dossier published in OGST Journal, Vol. 70, No. 2, pp. 215-390 and available online here

Cet article fait partie du dossier thématique ci-dessous publié dans la revue OGST, Vol. 70, n°2, pp. 215-390 et téléchargeable ici

DOSSIER Edited by/Sous la direction de : **B. Dewimille**

Fluids-Polymers Interactions: Permeability, Durability
Interactions fluides polymères : perméabilité, durabilité

Oil & Gas Science and Technology – Rev. IFP Energies nouvelles, Vol. 70 (2015), No. 2, pp. 215-390

IFP Energies nouvelles

Oil & Gas Science and Technology – Rev. IFP Energies nouvelles, Vol. 70 (2015), No. 2, pp. 251-266

DOI: 10.2516/ogst/2013198

Dossier

Fluids-Polymers Interactions: Permeability, Durability
Interactions fluides polymères : perméabilité, durabilité

Diffuso-Kinetics and Diffuso-Mechanics of Carbon Dioxide / Polyvinylidene Fluoride System under Explosive Gas Decompression: Identification of Key Diffuso-Elastic Couplings by Numerical and Experimental Confrontation

Jean-Claude Grandidier[1], Cédric Baudet[1], Séverine A.E. Boyer[1]*, Marie-Hélène Klopffer[2] and Laurent Cangémi[2]

[1] *Institut Pprime UPR 3346 / CNRS - ISAE-ENSMA, 1 Av. Clément Ader, 86961 Futuroscope - France*
[2] *IFP Energies nouvelles, 1-4 avenue de Bois-Préau, 92852 Rueil-Malmaison - France*
e-mail: severine.boyer@ensma.fr

* Corresponding author

Abstract — *The work aims at identifying the key diffuso-elastic couplings which characterize a numerical tool developed to simulate the irreversible 'Explosive Decompression Failure' (XDF) in semi-crystalline polymer. The model proposes to predict the evolution of the gas concentration and of the stress field in the polymer during the gas desorption [DOI: 10.10161j.composi-tesa.2005.05.021]. Main difficulty is to couple thermal, mechanical and diffusive effects that occur simultaneously during the gas desorption. The couplings are splitting into two families:*

- *indirect coupling (*i.e., *phenomenology) that is state variables (gas concentration, temperature, and pressure) dependent;*
- *direct coupling, (*i.e., *diffuso-elastic coupling) as polymer volume changes because of gas diffusion.*

The numerical prediction of the diffusion kinetics and of the volume strain (swelling) of PVF_2 (polyvinylidene fluoride) under CO_2 (carbon dioxide) environment is concerned. The prediction is carried out by studying selected combinations of couplings for a broad range of CO_2 pressures. The modeling relevance is evaluated by a comparison with experimental transport parameters analytically identify from solubility tests.

A pertinent result of the present study is to have demonstrated the non-uniqueness of the coefficients of diffusion (D) and solubility (S_g) between the diffuso-elastic coupling (direct coupling) and indirect coupling. Main conclusion is that it is necessary to consider concomitantly the two types of couplings, the indirect and the direct couplings.

Résumé — **Cinétique de diffusion et comportement diffuso-mécanique du système dioxide de carbone / polyfluorure de vinylidène sous décompression explosive de gaz : identification des couplages diffuso-élastiques majeurs par confrontation numérique et expérimentale** — Cette étude a pour objectif d'identifier les couplages diffuso-élastiques majeurs qui entrent en jeu dans une

modélisation des mécanismes irréversibles « d'Endommagement par Décompression Explosive de gaz » (EDE) des matériaux polymères semi-cristallins. Le modèle prédit l'évolution de la concentration en gaz et les champs de contraintes dans le matériau au cours de la désorption de gaz [DOI: 10.10161j.compositesa.2005.05.021]. La difficulté principale est de coupler les effets thermiques, les champs de contraintes et la diffusion du gaz qui se produisent simultanément au cours de la désorption. Les couplages sont classés selon deux familles :

– couplage indirect (phénoménologie) qui dépend des variables d'état (concentration en gaz, température et pression) ;
– couplage direct (ou couplage diffuso-élastique) pour lequel le volume du polymère évolue du fait de la diffusion du gaz.

La prédiction numérique des cinétiques de diffusion et des contraintes volumiques (gonflement) du PVF_2 (polyfluorure de vinylidène) sous environnement de CO_2 (dioxyde de carbone) est étudiée à travers une combinaison des couplages dans une large gamme de pressions en CO_2. La pertinence du modèle est évaluée par confrontation avec les paramètres de transport qui ont été évalués selon la procédure 'analytique conventionnelle' à partir des mesures expérimentales de solubilités.

Le résultat pertinent est d'avoir démontré la non-équivalence des coefficients de diffusion (D) et de solubilité (S_g) entre le couplage diffuso-élastique (couplage direct) et le couplage indirect. Une bonne modélisation du comportement diffuso-élastique du polymère nécessite la considération concomitante des deux familles de couplages, direct et indirect.

INTRODUCTION

Thanks to their good barrier properties, polymer materials are encountered in the pressure sheath of flexible oil-carrying pipes. With respect to the transported hydrocarbons, the permeability to corrosive gases, such as hydrogen sulphide (H_2S) or carbon dioxide (CO_2), must be sufficiently low to minimize the corrosion of the metal reinforcements; the metal reinforcements ensure the mechanical resistance of the pipes structure. However, the polymer materials are not fully impermeable to gases [1-3]. The loss of barrier task is accentuated in the case of sharp-pressure variations generating thus irreversible 'explosive' deterioration of the polymeric structures. The phenomenon is called 'Explosive Decompression Failure' (XDF) [4-6]. Various forms of damage appear, *i.e.*, cracks, blisters or structure-like foams within the polymer. The irreversible damage appears because of strong thermo-diffuso-mechanical couplings.

By considering especially the transport properties of carbon dioxide (CO_2) into polyvinylidene fluoride (PVF_2), the gas diffusion and solubility coefficients in the petroleum exploitation sheath cannot be determined through experiments because of the size of the sheath. As a result, it becomes of prime importance to use representative specimens and to propose modeling tools allowing the prediction of polymer behavior under real conditions of use. Several studies relating to the transport phenomena of gas into polymer have made it possible to establish the gas diffusion law and to evaluate the solubility with the swelling of various gas/polymer systems for various pressures and temperatures. Adapted accordingly, a non-exhaustive bibliographic review is presented below on CO_2/PVF_2 systems.

The mathematical theory of diffusion [7-10] for an isotropic system is based on the assumption of proportionality between the flux $\vec{J}$ of diffusing substance and the concentration gradient $\vec{\nabla}C$ through an elementary surface (C in ppm). The first Fick's law is expressed in Equation (1). D is called the diffusion coefficient (D in length^2.time^{-1}):

$$\vec{J} = -D\vec{\nabla}C \tag{1}$$

This first law is applicable for example in the steady state reached when the gas concentration in a membrane does not vary with time and the flux is constant. In transient state, the matter transfer by diffusion is different from zero and the penetrant concentration is a function of position and time. The second Fick's law of diffusion describes this non-steady state as expressed in Equation (2):

$$\frac{dC}{dt} = -div\vec{J} \tag{2}$$

The diffusion parameter D is a non constant characteristic of the gas/polymer system. When the interactions

between the polymer chains and the gas molecules are high (*i.e.*, CO_2 diffusion through fluoride polymers) the diffusion coefficient depends on the gas concentration inside the material. Within the general framework of gas/polymer systems, a relation of the type connects the diffusion coefficient to the thermodynamic variables (T, temperature; p, gas pressure) of the system as given in Equation (3):

$$D = D(C, T, p) \tag{3}$$

These dependencies of D state the various chemical affinities between gas and polymer. These phenomenological couplings were named indirect couplings [5].

For systems in which the solubility essentially obeys to the Henry's law (*i.e.*, hydrocarbons in elastomers), the dependence of the diffusion coefficient on the sorbed penetrant concentration has been empirically represented, for a given temperature, by linear Equation (4) and exponential Equation (5) [11-14]:

$$D(C) = D_0(1 + \beta C) \qquad \text{Linear model} \tag{4}$$

$$D(C) = D_0 \exp(\beta C) \qquad \text{Exponential model} \tag{5}$$

Equation (5) is used when the dependence on concentration becomes important. D_0 is the limit of D when the concentration C tends to zero (D_{long}). β is a constant parameter and is temperature dependent. If β is zero, the model corresponds to Fick's laws, Equations (1, 2), where D stays constant. These models have been considered in the works of Benjelloun-Dabaghi [15].

For systems in which the solubility does not exactly obey to the Henry's law but rather than an isotherm of Flory-Huggins type (*i.e.*, highly soluble gases in rubbery polymers), the concentration dependence of D can be represented consistently with Equation (6) [16-18]:

$$D(C) = D(0) \exp\left(\frac{\beta C}{1 + \sigma C}\right) \tag{6}$$

At a given temperature, σ is a constant related to penetrant/polymer interactions. Fujita *et al.* [19] have proposed a similar relationship from considerations based on the free volume theory.

The effect of pressure on gas diffusion through rubbery polymers has been studied to develop membranes useful of service for gases separation. Stern *et al.* [20, 21] concluded that the pressure influence could be explained as the result of two opposite phenomena. In the first effect, the hydrostatic pressure leads to an increase of the polymer density and thus to a reduction of polymer free volume. In the second effect, the increase in pressure induces a concentration enhance of molecules diffusing within the matrix. The diffusion in turn plasticizes the macromolecular chains involving a larger free volume. Naito *et al.* [22, 23] have studied the permeability of a series of pure gases into polymers in the rubbery state, such as polyethylene, polypropylene, and polybutadienes. The effect of gas pressure was carried out up to 10 MPa. To discriminate the two antagonistic effects, *i.e.*, hydrostatic constraint and plasticization, for a given temperature the dependency of the diffusion coefficient with pressure has been proposed as expressed in Equation (7):

$$D(C, p) = D(0, 0) \exp(\beta_h p - \alpha C) \tag{7}$$

$D(0, 0)$ is the diffusion coefficient at atmospheric pressure and for zero penetrating gas concentration. The term $\exp(\beta_h p)$ is the hydrostatic pressure effect. β_h is a negative coefficient expressing the reduction diffusion abilities of the material under pressure. The term $\exp(\alpha C)$ indicates the number of molecules increase dissolved into the polymer and giving rise to plasticization.

For higher pressures, beyond 20 MPa, Equation (7) is extended as concentration, temperature, and pressure dependent [15, 24]. The diffusion coefficient D is then expressed in Equation (8):

$$D(C, T, p) = D_0(T, p) \exp(\beta C) \tag{8}$$

In Equation (8), only the diffusion through the thickness of a membrane is considered. The parameters D_0 and β have been identified for various level of pressure for a given temperature. But most probably, to correctly evaluate this model, it would have been preferable to identify the parameters on one test and to validate them on the others.

The models of gas diffusion in the open literature are greatly established on couplings focused on the dependencies of D on concentration, pressure and temperature. However, solubility tests carried out on CO_2/PVF_2 system show the existence of a high diffuso-mechanical coupling. This coupling results in an important swelling of the material during the sorption stage, 40% for a pressure of 100 MPa, as it will be described further in the experimental investigation (*Sect. 2.1*).

As a result, the polymer elastic contribution (*i.e.*, mechanical response dues to volume change) to the diffusion phenomena becomes of the utmost importance [6]. Moreover, considerable hydrostatic, and so mechanical, pressure induces complex stress fields within the polymeric material especially under the high pressures constraints. This additional complexity must be added

in the analysis of the couplings between mechanical and diffusion phenomena.

To date, a body of models tentatively describes the existence of strong couplings between mechanical, thermal and diffusive phenomena occurring in polymeric materials in fluid transport, with the additional difficulty in modeling the state of the fluid within the polymer. Theoretical descriptions of these coupling phenomena are based on empirical or thermodynamic interpretations, as given in the selected open literature [25-37].

As an attempt, Rambert *et al.* [5, 32-34] described the effect of gas on the mechanical behavior of material through diffuso-mechanical coupling, as it will be explained in Equation (10). The diffuso-mechanical coupling is classically defined by an isotropic expansion coefficient linked to gas concentration. In this modeling, the CO_2/PVF_2 system has been considered as a mixture for which the molecular diffusion obeys to the laws' Fick, Equations (1, 2). The originality of Rambert *et al.* [5, 32–34] approach consists in the addition of a coupling term, due to the gradient of the elastic volume strain, to the divergence of the substance diffusing flux as was given in Equation (2). The additional terms in Equations (10, 12), presented in Section 2, are named direct couplings. The chosen method has been to systematically eliminate the indirect couplings, as described previously, in order to evaluate the effect of the direct couplings. This model has been applied to a structure subjected to an explosive decompression, and a parametric study showed the implication of the direct couplings during stages of transition.

From a purely mechanical point of view, one can see that two types of couplings appear, direct and indirect. The indirect couplings were validated in a majority of system having diffusion kinetics at the mercy of pressure, concentration and/or temperature. Nevertheless, they are not enough to describe the volume strain induced by the sorption of a gas into a polymer. The direct couplings can be used to describe concomitantly the diffusion kinetics and the mechanical behavior of a polymer subjected to a gas diffusion. The indirect couplings outline the dependency of the transport parameters on the state variables; indirect means that these couplings can be substituted into the direct couplings, which involve the transport parameters. All these couplings must be evaluated, in particular to improve the analysis of the experimental tests and for a more accurate modeling of the basic phenomena involved during the sorption and the diffusion of gas into polymer.

Consequently, the present work aims at studying the relevance and the limits of these couplings by using the formalism of the thermodynamics on the example of CO_2/PVF_2 system. A first discussion was introduced in our previous work [35]. In the diffusion problem, see the following Equations (11, 12), the formalism of the thermodynamics is described within two parameters, k_μ (a coupling parameter related to the effect of the chemical potential gradient on the gas mass flux) and α_c (the isotropic expansion coefficient related to mass transport). A new identification of the diffusion problem, dependent on the polymer volume variation and gas concentration in the polymer, is proposed by numerically quantifying the parameters k_μ and α_c of the direct couplings.

This article is organized into three parts. In Section 1, a brief presentation of the indirect couplings proposed by Rambert *et al.* [5, 32–34] is presented. Section 2 describes the experimental solubility tests. These tests permit to determine the transport parameters of CO_2 in PVF_2. The mass and the volume of (gas + polymer) mixture are measured during gas desorption at a given temperature and various pressures levels. For any level of pressure, desorption can be decomposed into two phases: a first phase of decompression during which it can be supposed that temperature fluctuations do not notably influence diffusion when compare to the effect of concentration, and a second phase at atmospheric pressure and constant ambient temperature for which measurements have been done. The couplings with thermal phenomena are neglected; only the diffuso-mechanical couplings during gas desorption are studied. Two pressures ranges are of interest. At low pressures tests (0.5, 1.5 and 4 MPa), only the mass have been measured after gas decompression. At high pressures tests (25, 50 and 100 MPa), the mass and the volume have been measured. In Section 3, the ability of the various types of couplings is studied to predict the diffusion kinetics and the volume strain of CO_2/PVF_2 system. Experimental measurements and computed values are compared. In a first attempt, the study of indirect couplings is examined. We estimate the effect of pressure and gas concentration in the polymer with linear and exponential dependencies of the diffusion coefficient, Equations (4, 5); the volume change is considered explicitly as well as the gradients effects of the volume deformation due to the sorption stage. In a second attempt, the study of diffuso-elastic direct coupling is carried out, Equation (12). In both the attempts, the high pressures tests are studied because the polymer volume evolution is known for such tests. By using a constant diffusion coefficient adapted at each level of pressure of the solubility test, the expansion coefficient related to the diffusion is determined in order to obtain the maximum swelling of the specimen at equilibrium. The effect of the hydrostatic compression of the polymer is compared to the plasticizing effect of gas, Equation (7).

Finally, the coupling with the elastic volume strain in the diffusion law is evaluated and compared with the effect of the gas concentration.

1 DIFFUSO-MECHANICAL MODEL: DIRECT COUPLINGS

The direct couplings are described according to the thermo-diffuso-elastic-linear approach of Rambert *et al.* [5, 32-34]. The thermal couplings are neglected and only the diffuso-elastic couplings are retained. This model has been developed in the framework of the generalized standard media, and therefore follows a classical approach. In this thermodynamic frame, the Elementary Representative Volume (ERV) describes a bi-component, continuous, homogeneous medium: polymer and gas, at a macroscopic scale. The introduction of a first potential (specific free energy) defines the laws connecting the thermodynamic forces (stress, chemical potential) with dual variables (strain $\underline{\underline{\varepsilon}}^e$, gas concentration C). With the assumption of small perturbations, *i.e.*, small strain and small difference of gas concentration, the Taylor expansion of this potential up to the second order leads to linear coupled constitutive equations.

The dissipations, which are only associated with the diffusion phenomenon in the elastic case, are obtained by using a second potential, *i.e.*, dissipation potential. The dissipation potential depends on the coupling phenomena which are taken into account. Once these are defined, under the assumption of uncoupling between dissipative phenomena, a complementary evolution law is obtained, Equations (11, 12). It is to be noted that the model was developed by prescribing constant values for all the material parameters.

By considering the previous assumptions, the diffuso-elastic model is finally defined *via* a mechanical problem and a problem of diffusion [35] under the following forms:

– Mechanical problem:

$$\vec{div}\,\underline{\underline{\sigma}} + \rho\vec{f} = \vec{0} \tag{9}$$

$$\underline{\underline{\sigma}} = \underline{\underline{\sigma_0}} + \lambda\left(tr\underline{\underline{\varepsilon}}^e\right)\underline{\underline{I}} + 2\mu\underline{\underline{\varepsilon}}^e - (3\lambda + 2\mu)\alpha_c\,(C - C_0)\underline{\underline{I}} \tag{10}$$

$\underline{\underline{\sigma}}$ is the total Cauchy stress tensor (Pa) applied to the CO_2/PVF_2 mixture. ρ is the average mixture density (kg.m^{-3}). $\vec{f}$ is the body force per unit mass (N.kg^{-1}) at any point within the ERV. $\underline{\underline{\sigma_0}}$ and C_0 represent the initial stress (Pa) and gas concentration (cm^3 (STP). cm^{-3}), respectively. λ and μ are the Lamé elastic coefficients (Pa). α_c is the isotropic expansion coefficient related to mass transport. $\underline{\underline{I}}$ is the identity matrix;

– Diffusion problem:

$$\frac{dC}{dt} = -div\,\vec{J} \tag{11}$$

$$\vec{J} = -D(\vec{\nabla}C) - k_\mu\frac{10^6(3\lambda + 2\mu)\alpha_c}{\rho^2}\left(\vec{\nabla}\left(tr\underline{\underline{\varepsilon}}^e\right)\right) \tag{12}$$

k_μ is a coupling parameter related to the effect of the chemical potential gradient on the gas mass flux (kg.s.m^{-3}). ε^e is the elastic volume strain and tr is the trace operator.

Equations (11, 12) convey couplings between diffusion and elastic phenomena. The first terms in the right hand side of Equation (10) are of the Hooke's law types. The last term corresponds to the effect of the gas diffusion on the mechanical behavior of the material. In a reciprocal way, in the diffusion law, Equation (12), the product ($k_\mu \times \alpha_c$) reflects the effect of the elastic volume strain ($tr\underline{\underline{\varepsilon}}^e$) on the evolution of the gas concentration in the material.

Added in the flux Equation (12), the phenomenological laws expressing the effects of concentration and pressure on the diffusion coefficients, see Equations (4, 5) or (8), have complemented this model. Consequently, the two types of couplings are present at various levels in the diffusion Equation (12).

For the various CO_2 Saturation Vapor pressures (SVps) considered in the present work, the sorption curve of the CO_2/PVF_2 system is supposed to follow the Henry's law [1, 7]. The Henry's law expresses the relationship between the applied pressure p (Pa) and the gas concentration C through a solubility coefficient S_g (cm^3 (STP).cm^{-3}.Pa^{-1}), as given in Equation (13):

$$C = S_g p \tag{13}$$

2 EXPERIMENTAL INVESTIGATION: SOLUBILITY TEST AND ANALYTICAL ANALYSIS OF DIFFUSION COEFFICIENTS

In the conduction of solubility tests, the evolutions of the mass and volume of CO_2-saturated PVF_2 during desorption are concerned. Mass measurements permit to define two transport parameters, the coefficients of solubility S_g and of diffusion D. Only the parameter D is studied. This parameter can be analytically calculated at the beginning and the end of desorption curves accordantly to two methods. The analytical analysis gives rise to two constant diffusion coefficients, namely D_{short} and D_{long}, related to the desorption curve. Discussion on both the diffusion coefficients is established.

2.1 Description of the Solubility Test – Experimental Results

The poly(vinyli-dene fluoride) PVF_2 investigated is a main component as efficient barrier against light fluids for making on-duty pipe-lines seals [38]. The polymer characteristics are found in [39]. It is a Kynar 50HD, a polymer without additives like plastifiants or elastomers. Melting temperature and cristallinity degree are 168°C and 48%, respectively. Purity of carbon dioxide CO_2 is given at 99.5% and used without further purification. Physical properties of CO_2 can be found in [38].

The solubility tests have been performed at IFP Energies nouvelles (IFPEN). They can be conducted according to two stages: sorption and desorption. A polymeric specimen is placed in a pressure cell [39, 40] thermally controlled. The pressure cell is connected to high pressure valves allowing the circulation of the gas. During the sorption stage, temperature and gas pressure are gradually increased, and then maintained constant until the specimen is fully saturated with gas. At low-pressure tests (0.5, 1.5 and 4 MPa), the sorption temperature is 313 K. At high-pressure tests (25, 50 and 100 MPa), the sorption temperature is 403 K. Heating the pressure cell reduces the saturation period in sorption phase. Indeed, for a given pressure, the diffusion coefficient is generally related to the temperature by an Arrhenius's law [41]. After saturation, the pressure cell, in which the polymer seats, is quenched with water until the temperature drops to 298 K by maintaining the pressure constant. During the desorption phase, a fast decompression to the atmospheric pressure is first achieved. Then, the sample is left out the pressure cell and the specimen volume is measured at regular time intervals under atmospheric pressure and at ambient temperature (the first measurement is carried out about 15 min after decompression).

The measurements of mass $m(t)$, volume $V(t)$ and density ρ of the specimen during desorption have been made by double weighing, in the ambient air and in immersion into ethanol. The uncertainty on measurements is 0.01 g. Archimedes' principle is used to calculate the volumes of the specimen during desorption. The immersion time (< 30 s) into ethanol is supposed to be sufficiently small so that the sample does not absorb it. The mass and the volume variations are calculated according to Equation (14):

$$\Delta M(\%) = 100\frac{m(t) - m(i)}{m(i)}$$
$$\Delta V(\%) = 100\frac{V(t) - V(i)}{V(i)} \quad (14)$$

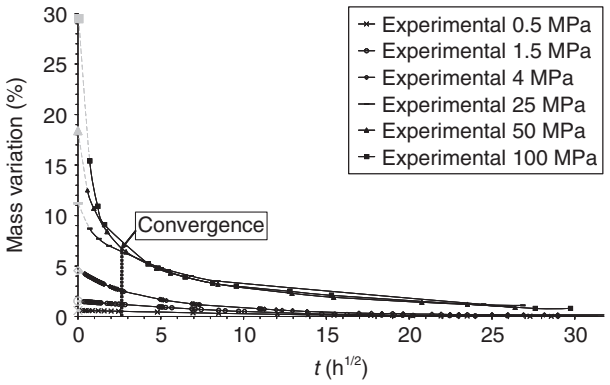

Figure 1

Experimental curves of desorption kinetics for low- and high-pressure tests.

$m(i)$ and $V(i)$ are the initial mass and volume of the specimen, respectively.

The solubility tests are conducted on a membrane with a square base ($m(i) = 4.44$ g, $V(i) = 2.56$ cm^3, thickness of 1.1 mm, and base length of 47 mm) for low pressures and on a ring shaped membrane ($m(i) = 7.62$ g, $V(i) = 4.37$ cm^3, thickness of 4.8 mm, and external and interior radius of respectively 25 and 10.5 mm) for high pressures [35]. The density of native PVF_2 is 1 745 kg.m^{-3}.

The mass evolutions during desorption for the six applied pressures are illustrated in Figure 1. Because of the high pressure amplitude between tests, the mass variation is plotted for the low pressure tests in a separate Figure 2. The first point of each curve, in grey, corresponds to the extrapolation at zero time of the desorption curve. Extrapolation is carried out by using a polynomial function of degree 4 on the first four points of each curve. This kind of representation is preferred to the graphs plotted classically in literature by normalizing the mass because it makes more easily to represent a broad range of pressures. However, it can also loose some information. For example, at the highest pressures, after approximately nine hours of desorption, a convergence point appears in the mass variation curves, contrary to the normalized mass curves. For the test investigated at 4 MPa, it seems that a residual CO_2 mass exists in the membrane (*Fig. 2*). Indeed, for the low-pressure tests at 0.5 and 1.5 MPa, the sample recovers its initial mass at the end of desorption, whereas at 4 MPa it remains approximatively 0.13% of gas in the membrane (approximatively 6 mg of gas). For the high-pressure tests (*Fig. 1*), we can think that a residual

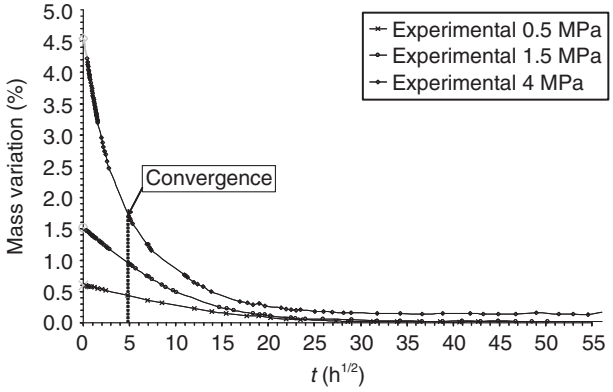

Figure 2

Experimental curves of desorption kinetics for low-pressure tests.

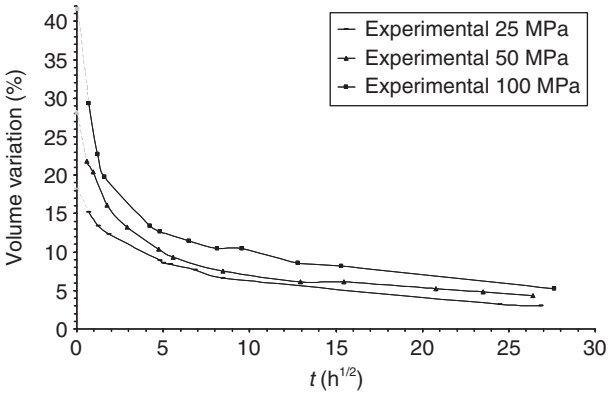

Figure 3

Experimental curves of volume variations during CO_2 desorption in PVF_2 for high-pressure tests. (Reprinted from [35], *Fig. 1*).

quantity of gas of approximately 0.8% remains in the ring (approximatively 60 mg of gas).

The volume evolution of the ring for the high-pressure tests is plotted in Figure 3. In the same way as a residual quantity of gas seems to stay in the sample, a residual volume strain of approximatively 4% is noticed. At the end of measurements, the density of the samples is always lower than the initial density. This remark can be correlated with the macroscopic observations carried out during desorption which suggest that sudden blisters appear within the material.

Contrary to mass desorption kinetics, a not clear convergence point appears in volume variation kinetics (*Fig. 3*); but the mass and volume evolution curves during desorption follow the same tendency. Indeed,

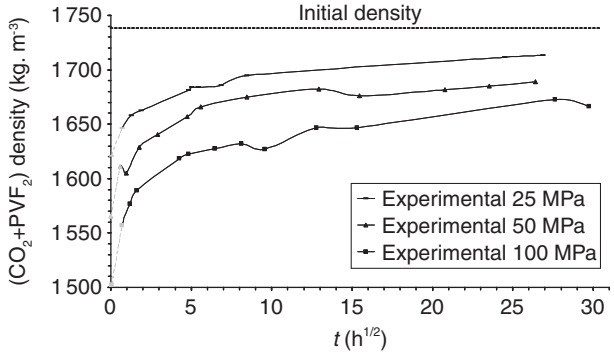

Figure 4

Experimental density variations of the (CO_2 + PVF_2) mixture during desorption for high-pressure tests.

Figure 4 shows that, with the exception of the beginning of desorption (decompression phase), the mass of the (dissolved gas + polymer) mixture decreases linearly with the volume. Consequently, this material is appropriate for discussing the diffuso-mechanical coupling model pointed out previously.

2.2 Analytical Evaluation of the Diffusion Coefficient

When a membrane of polymer is immersed in a penetrant, the concentration C in the material is given, at time t, by the solution of the second Fick's law, Equation (2), with a constant diffusion parameter, assuming that during desorption the gas diffuses only in the thickness direction, *i.e.*, in one-dimension (1-D) [41-43]:

$$\frac{C}{C_{\max}} = 1 - \frac{4}{\pi}\sum_{n=0}^{\infty}\frac{(-1)^n}{(2n+1)}\exp\left(\frac{-D(2n+1)^2\pi^2 t}{4l^2}\right) \times \cos\left(\frac{(2n+1)\pi x}{2l}\right) \tag{15}$$

$2l$ denotes the membrane thickness. The sample centre is located at $x = 0$. $C_{\max}$, the gas concentration in contact with the membrane faces, is considered as immediately prescribed. This equation does not take into account the diffusion towards the edges of the membrane, as far as, in this system, the membrane thickness is very small compared to the other dimensions. In the Fick's law the volume change is not taking into account.

Equation (15) can be integrated to obtain the mass of penetrant, M, absorbed by the sample at time t, assuming that temperature and pressure stay constant

[41-45]. M_{max} represents the mass of the diffusing species absorbed by the material at equilibrium, l stands for the membrane thickness [8].

$$\frac{M}{M_{max}} = 1 - \sum_{n=0}^{\infty} \frac{8}{(2n+1)\pi^2} \exp\left(\frac{-D(2n+1)^2\pi^2 t}{l^2}\right) \quad (16)$$

Based on the desorption equation, Equation (16), two 'conventional' analytical methods, called 'short time method' and 'long time method', are used to determine the diffusion coefficients at the beginning and at the end of the desorption [39]. The analytical values of D_{short} and D_{long} are given in Table 1.

2.2.1 Analytical Determination of the So Called `Short Time Diffusion Coefficient' D_{short}

D_{short} predicts the beginning of the experimental desorption curve. Its identification makes use of the extrapolated point as previously defined by the polynomial function of degree 4. The first part of the experimental curve assumes to obey to a semi-infinite diffusion law. Moreover, presuming that the diffusion corresponds to a Fickian behavior, the curve M/M_{max} *versus* $t^{1/2}/l$ is linear between 1 and 0.5. In that case, the value of t/l^2 for which the ratio M/M_{max} equals ½ is expressed by Equation (17) and D_{short} is given by Equation (18) [8]:

$$\left(\frac{t}{l^2}\right)_{\frac{1}{2}} = -\left(\frac{1}{\pi^2 D}\right) \ln\left(\frac{\pi^2}{16} - \frac{1}{9}\left(\frac{\pi^2}{16}\right)^9\right) \quad (17)$$

$$D_{short} = \frac{0.04919}{\left(\frac{t}{l^2}\right)_{\frac{1}{2}}} \quad (18)$$

2.2.2 Analytical Determination of the `Long Time Diffusion Coefficient' D_{long}

D_{long} predicts the end of the experimental desorption curve. When M/M_{max} is lower than 0.4, the desorption equation can be written as Equation (19). K is a constant value:

$$\ln\left(\frac{M}{M_{max}}\right) = \ln\left(\frac{K}{\pi^2}\right) - \left(\frac{D\pi^2 t}{l^2}\right) \quad (19)$$

By plotting $\ln(M/M_{max})$ as a function of time t, the end of this curve is nearly a straight line whose slope can be used to calculate the parameter D_{long} as given in Equation (20):

$$D_{long} = -\frac{l^2(slope\ coefficient)}{\pi^2} \quad (20)$$

2.2.3 Comments about the conventional analytical evaluation

The diffusion coefficient D_{short} highly depends on the first point of the semi-infinite desorption curve. This point is estimated by extrapolating the desorption curve since the decompression starts. Consequently, if this point is overestimated, the coefficient D_{short} overestimates the beginning of the desorption kinetics. Conversely, if this point is underestimated, the coefficient D_{short} underestimates the beginning of the desorption kinetics. Even, the accuracy of the coefficient D_{long} is low because the assessment of the slope in Equation (20) depends on the number of points experimentally acquired.

D_{short} and D_{long} coefficients increase when the applied pressure rises. So, when the applied pressure is high, the slope of desorption curve, at a given time, increases

TABLE 1

Diffusion coefficients D_{short} and D_{long} calculated with the analytical method and the numerical simulations

Pressure (MPa)		0.5	1.5	4	25	50	100
$(m^2.s^{-1})$ $(\times 10^{-12})$	D_{short} (analytical)	0.216	0.409	1.95	30	111	246
	D_{short} (numerical simulation)	0.145	0.30	2.42	90	180	360
	D_{long} (analytical)	0.12	0.21	0.12	0.5	1.0	2.5
	D_{long} (numerical simulation)	0.10	0.10	0.10	1.5	1.5	1.5

TABLE 2
Solubility coefficient (ppm.Pa^{-1}) at different pressures for the CO_2/PVF_2 system

Pressure (MPa)	0.5	1.5	4	25	50	100
$(S_g)_p$ (ppm.Pa^{-1}) ($\times 10^{-2}$)	1.20	1.0	1.07	0.405	0.311	0.229

(*Fig. 1*). Moreover, for a given level of pressure, the necessity to use two diffusion coefficients in order to describe at best the desorption kinetics means that the parameter D depends on the gas concentration in the material.

It assesses the necessity to study the influence of gas pressure and gas concentration on the diffusion coefficients D, Equations (4, 5) and (8). This analysis can be carried out by using optimizing methods [15] or by numerically simulating the test of solubility. This later numerical alternative consists in carrying out a parametric study of D by numerically simulating the solubility test with the Fick's law. In Section 3, the comparison of the results of these two analytical and numerical methods makes it possible to conclude on their abilities to evaluate the diffusion parameters at the beginning and the end of desorption.

3 NUMERICAL SIMULATION OF THE BEHAVIOR OF PVF_2 WITH CO_2: IDENTIFICATION OF KEY COUPLINGS

To numerically simulate the diffuso-mechanical behavior of the CO_2/PVF_2 system, the two types of couplings are considered, namely the direct couplings, Equations (9-12), and the indirect couplings, Equations (4, 5). These laws have been implemented into the engineering finite element code Abaqus^{TM} by means of an User ELement (UEL) subroutine, as applied in [32-37]. To simulate the couplings, it is used 9 000 finite elements defined in the UEL with 20 nodes and 27 integration points. Details can be found in [35-37].

This tool gives the volume evolution of the sample and the gas concentration in the sample during the solubility test. The following Equation (21) expresses the mass of the gas in terms of its gas concentration C, $m(i)$ represents the initial mass of the specimen:

$$mg = \frac{10^{-6} C m(i)}{1 - 10^{-6} C} \tag{21}$$

To optimize the computing time, only a quarter of the membrane with a square base and one section of the ring have been modeled by taking into account the appropriate symmetries. As regards the loading and the boundary conditions, they have been defined so as to reproduce the experimental test conditions, *i.e.*, a sample placed on a porous support in a pressure cell and subjected to a variation of pressure and temperature. The contact between the sample and the porous support has not been modeled in a refined way during the simulation in order to minimize the difficulty of the study.

Properties of the native PVF_2 at 21°C are a Poisson's ratio of 0.38 and a Young modulus of 1 743 MPa [5]. The value chosen for the solubility coefficient is that obtained experimentally at IFPEN (*Tab. 2*). In the Abaqus^{TM} code, the solubility parameter is expressed in ppm.Pa^{-1}.

In the parametric study, the three unspecified parameters are the diffusion coefficient D, and the direct coupling parameters, α_c and k_μ. The concentration and pressure dependencies, Equations (4, 5) and (8), are first studied neglecting thus the direct couplings (*i.e.*, $\alpha_c = k_\mu = 0$). Then, the effect of the diffuso-elastic couplings on the desorption kinetics and on the mechanical behavior of the material is investigated by using a constant diffusion coefficient adapted at each level of pressure. Finally, this study compares these two kinds of coupling and concludes on the type of coupling that must be used so as to characterize as well as possible the behavior of the PVF_2 subjected to a CO_2 pressure fluctuation.

3.1 Parametric Evaluation of the Indirect Couplings – Influence of Pressure and Concentration on the Diffusion Coefficient

The indirect couplings describe the mass evolution of a specimen during a solubility test, but not explicitly the evolution of specimen volume. So, only the diffusion kinetics is considered in this paragraph.

First of all, due to the uncertainty of the analytical methods to precisely determine the diffusion coefficients D_{short} and D_{long} as previously discussed, a numerical identification of the two parameters is performed at each level of pressure of the solubility tests. The simulations are achieved to minimize the experience/model difference and to identify the diffusion coefficients without hypothesis. The minimization solves the problem of diffusion in three-dimension (3-D, Abaqus^{TM}) without imposing any direction on diffusion flux. It uses the

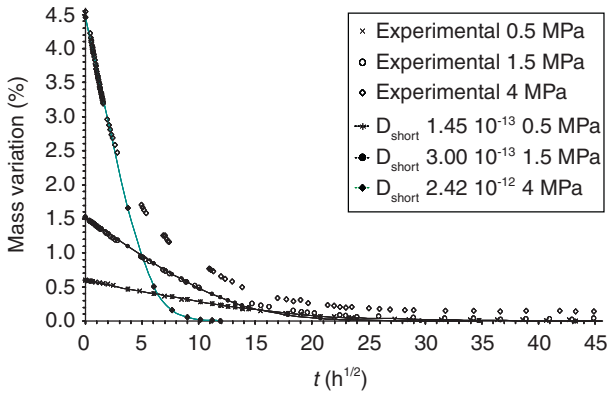

Figure 5

Desorption kinetics, with parameter D_{short} and Fick's law for low-pressure tests.

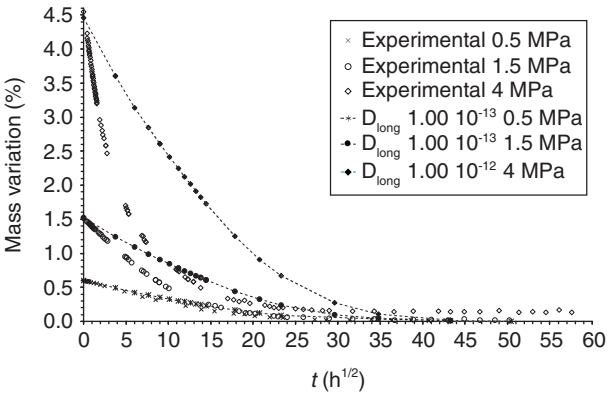

Figure 7

Desorption kinetics, with parameter D_{long} and Fick's law for low-pressure tests.

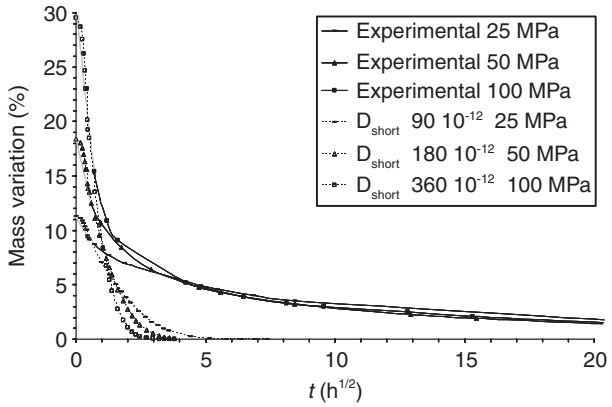

Figure 6

Desorption kinetics, with parameter D_{short} and Fick's law for high-pressure tests.

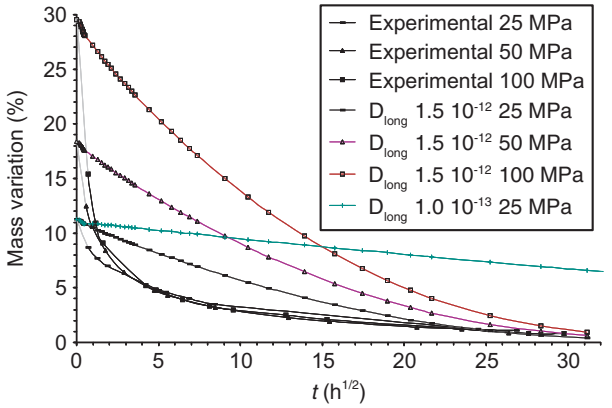

Figure 8

Desorption kinetics, with parameter D_{long} and Fick's law for high-pressure tests.

classical diffusion element defined in Abaqus™ by means of the Fick's law. This parametric method permits to reproduce as well as possible the beginning and the end of the desorption kinetics by searching appropriate values of D_{short} (*Fig. 5*, *6*) and D_{long} (*Fig. 7*, *8*). The new diffusion coefficients can be compared with those previously obtained thanks to the analytical methods (*Tab. 1*).

The analytical values with the numerical values remain in the same order of magnitude (10^{-12} $m^2.s^{-1}$). For low-pressure tests, lower than 1.5 MPa, D_{short} has certainly been overestimated by the analytical method whereas for the other pressures it has been underestimated. These discrepancies notably stem from the rough extrapolation at the initial time of the experimental desorption curve. So, even if the analytical method can be used to quickly obtain the diffusion coefficients at the beginning and the end of desorption, the numerical simulation seems to be more suitable to determine these parameters in a more precise way.

At the end of desorption, the diffusion coefficient should be the same for the different pressures. The results obtained with these two methods show that it is necessary to use two diffusion coefficients to fit the end of the desorption kinetics: one for the low-pressure tests and another one for the high-pressure tests, higher than the first. This result is confirmed as illustrated in Figure 8 by simulating the solubility test at 25 MPa with the same D_{long} diffusion coefficient as that of the low pressure tests (*Tab. 1*). In order to understand this change in behavior, the following assumption is put forth. The temperature during the sorption phase is not the same for low-pressure tests (313 K) and for

high-pressure tests (403 K). A strong reorganization of matter (*i.e.*, molecular chains) is thus possible during sorption at 403 K. However, decompression is preceded by a quenching during which the polymer, perhaps, does not have time to relax to its initial state of equilibrium. Moreover, diffusion increases with temperature [17]; it is thus possible that the polymer behavior after quenching is equivalent to its behavior at 403 K, explaining a faster desorption for high pressures than for low pressures.

The diffusion parameter D_{short} seems to increase whatever the characterization method when the applied pressure rises. For pressures higher than 0.5 MPa, this dependency on pressure does not make it possible to obtain the whole desorption kinetics (*Fig. 5*). Undeniably, due to this dependency, for pressures higher than 1.5 MPa, only the beginning of the desorption curve with a diffusion coefficient D_{short} (*Fig. 5*, *6*) or its end with a diffusion coefficient D_{long} (*Fig. 7*, *8*) can be obtained. The experimental desorption curve lies between the two desorption curves simulated with the Fick's law and using the parameters D_{short} and D_{long}, respectively. So, during desorption, the coefficient D decreases from D_{short} to D_{long}. Consequently, beyond 0.5 MPa in which Fick's law is sufficient to describe the desorption phase of a solubility test, the effect of concentration on the diffusion parameter D becomes not negligible.

Linear and Exponential Diffusion Laws

In order to study the dependence of the diffusion coefficient with gas concentration, linear Equation (4) and exponential Equation (5) diffusion laws are incorporated into the Rambert's subroutine UEL [5, 32-34].

For the pressures of 1.5 and 4 MPa, the solubility tests are simulated with the linear law by using the diffusion coefficient D_{long} obtained at these pressures as a value for the parameter D_0, *i.e.*, 1×10^{-13} m^2.s^{-1}. A parametric study with subroutine UEL has been performed to determine the parameter β that induces the best prediction of the beginning of the experimental desorption curve. This parameter has the same value for the two pressures and is taken as 3×10^{-4} (*Fig. 9*). With these parameters, only the end of desorption curve at 4 MPa is not correctly predicted, probably because of gas trapped in the material. These results show that a linear dependence is sufficient to correctly model the diffusion behavior of the PVF_2 for CO_2 pressures up to 4 MPa.

The same type of simulation is carried out for the high pressures tests by applying the linear and exponential laws. The diffusion coefficient D_{long} previously obtained for these tests is chosen as a value for the parameter D_0, *i.e.*, 1.5×10^{-12} m^2.s^{-1}. Numerical simulation results at

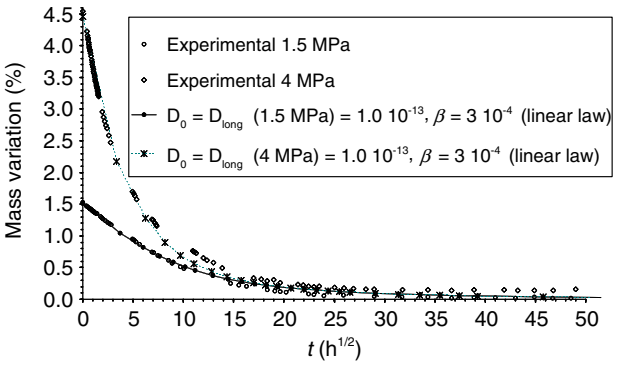

Figure 9

Desorption kinetics for low-pressure tests (1.5 and 4 MPa): linear laws for parameter D.

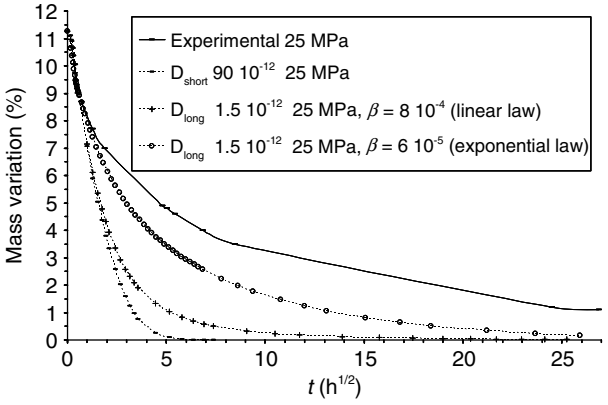

Figure 10

Desorption kinetics for a high-pressure test (25 MPa): comparison between Fick's law (D_{short} of 90×10^{-12} m^2.s^{-1}), linear and exponential laws (D_{long} of 1.5×10^{-12} m^2.s^{-1}).

25 MPa are illustrated in Figure 10; the numerical results are given for both linear and exponential laws. As well, Fick's law data previously calculated with a D_{short} of 90×10^{-12} m^2.s^{-1} are plotted (*Fig. 6*). The estimate of the beginning of desorption kinetics is improved by increasing the concentration dependency on mass variation (or diffusion coefficient). However, even by prescribing high dependencies on gas concentration, the experimental desorption curve cannot be completely predicted.

Similar numerical analysis executed at 50 and 100 MPa permits to express the dependence of the parameter β for each applied pressure by Equations (22, 23):

– for the Linear law:

$$\beta = 6 \times 10^{-4} \ln(p) - 1.1 \times 10^{-3}, \quad \forall 25 \leq p \leq 100 \text{ MPa} \tag{22}$$

– for the Exponential law:

$$\beta = -10^{-5} \ln(p) + 10^{-4}, \quad \forall 25 \leq p \leq 100 \text{ MPa} \tag{23}$$

These equations show that the gas concentration influence on the diffusion coefficient in CO_2/PVF_2 system is predominant at high pressures. These results also show that the classical laws of diffusion are insufficient to predict the desorption kinetics for the high pressures tests. To improve the evaluation of the diffusion of CO_2 in PVF_2, the knowledge of the thermodynamic state of the dissolved gas becomes point of interest [6]. That raises a fundamental problem and would direct further works.

In the following part, a first approach is proposed where the gas dissolved in polymer is described by a simple chemical potential [33].

3.2 Evaluation of the Direct Couplings

The objectives of the section are to describe the swelling of PVF_2 and to evaluate the effect of the direct couplings between the diffusion coefficient and gradient of elastic volume strain ($tr\underline{\underline{\varepsilon}}^e$), Equation (12), on mass variation.

Parametric Study of the α_c Expansion Parameter

The volume deformation of the samples in the tests at 0.5, 1.5 and 4 MPa has not been experimentally measured. Therefore, the α_c parameter study is restricted to high pressures. To obtain the α_c expansion parameter corresponding to the experimental volume strain threshold at the end of sorption, that is to say the simulation of the maximum swelling when the polymer is saturated by gas, high pressure tests are numerically simulated by uncoupling the diffusion phenomena Equation (12) ($k_\mu = 0$, $\alpha_c \neq 0$) and by using the diffusion coefficients D_{short} obtained previously with the numerical simulations (*Tab. 1*). The unique value of the α_c parameter equals 0.6 (*Fig. 11*) [35].

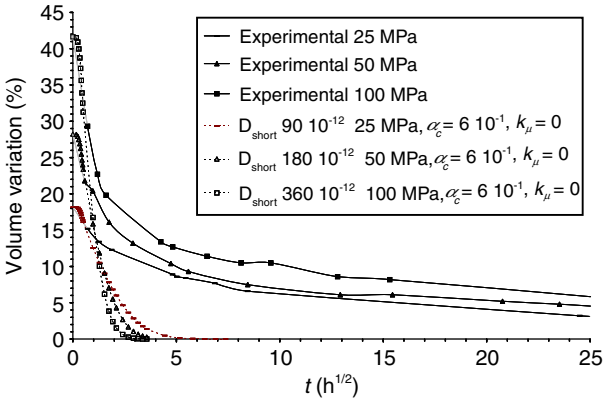

Figure 11

Volume variations, for high-pressure tests (25, 50 and 100 MPa), during CO_2 desorption in PVF_2 with D constant and a diffuso-elastic coupling (only the mechanical behavior).

By assuming that the membranes subjected to low pressures have the same behavior than those subjected to high pressures (*i.e.*, α_c is pressure independent (25 to 100 MPa)), their maximum volume strain can be calculated (*Tab. 3*) by using the above parameter α_c and by inverting the mechanical constitutive Equation (10). One must specify that in this model the diffusion coefficient does not have any effect on the value of the α_c parameter; this assumption will have to be validated during the experiments.

Parametric Study of the k_μ Coupling Parameter

For a constant diffusion coefficient, the diffusion kinetics is now modified by the diffuso-mechanical coupling which depends on the product of the k_μ and α_c parameters. By using the α_c coefficient, as previously defined, the effect of this coupling on desorption kinetics is then explored. Figure 12 compares the numerical simulations of the mass variation in the uncoupled case (*i.e.*, Fick's law) and in the case of direct couplings (*i.e.*, various products ($k_\mu \times \alpha_c$).

The coupling induces a strong deceleration of the desorption but is unable to account for the desorption kinetics. In fact this coupling is strongly related to the

TABLE 3

Maximum volume strain, at various pressures, calculated with parameter $\alpha_c = 0.6$

Pressure (MPa)	0.5	1.5	4	25	50	100
$\Delta V_{\max}$ (%)	1.08	2.7	7.7	18.2	28.2	41.6

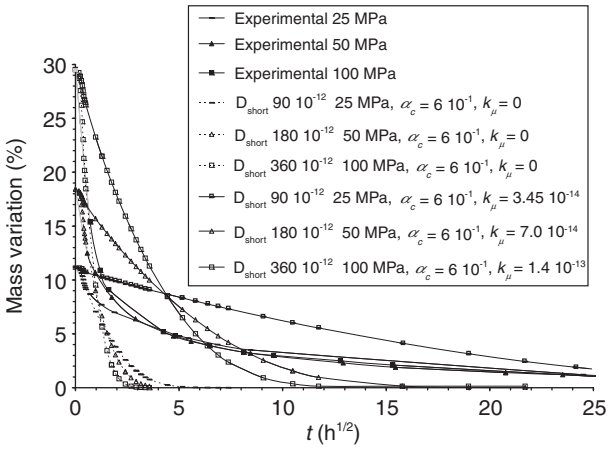

Figure 12

Desorption kinetics (mass variation), for high-pressure tests (25, 50 and 100 MPa), with constant D_{short} (*i.e.*, Fick's law) adapted at each level of pressure and a diffuso-elastic coupling (*i.e.*, various products $k_\mu \times \alpha_c$).

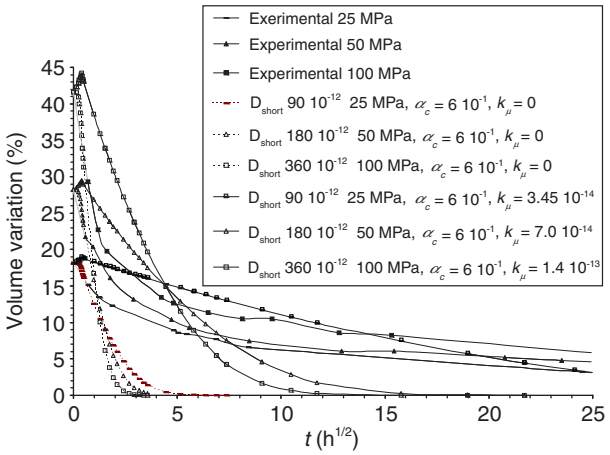

Figure 13

Volume variations, for high-pressure tests (25, 50 and 100 MPa), during CO_2 desorption in PVF_2 with constant D_{short} (*i.e.*, Fick's law) adapted at each level of pressure and a diffuso-elastic coupling (various products $k_\mu \times \alpha_c$).

gradient of the elastic volume strain, which is perhaps too small in the case of the solubility test studied here. In order to have a significant effect, a high value of k_μ is requisite.

Concerning the effect of the coupling on the volume variations during desorption (*Fig. 13*), the remarks are the same as for the mass evolution. The deceleration of the volume strain can be correlated with that of the desorption kinetics (*Fig. 12*).

Indeed, the increase in the sample size during sorption involves an increase in distance to be crossed by the gas molecules within the material. Thus, for a given diffusion coefficient, these molecules must spend more time to travel a given distance in the sample. The inverse effect occurs when the material contracts during desorption. In Figure 13, for a high coupling ($k_\mu = 3.45 \times 10^{-14}$), the sample volume continues to increase during decompression whereas the quantity of gas starts to decrease. It means that the contraction of the sample due to desorption does not compensate for the volume expansion related to the external pressure drop, because a high coupling induces an important deceleration of the diffusion of gas towards the outside. For example, at a pressure of 25 MPa, during decompression the increase by volume is 0.88%. This variation can be broken up into two parts. One is induced by the hydrostatic pressure drop which involves a volume increase by 1.03%, it is a purely mechanical effect. The other one is related to the contraction due to the desorption during the external pressure drop, it is the effect of the coupling between diffusion and mechanical phenomena. The latter is obtained by the difference between the total increase and that of mechanical origin, −0.15%. Then, as soon as the external pressure does not vary any more, the sample is subjected to the atmospheric pressure, and desorption involves the contraction of the sample (*Fig. 13*).

We now propose to predict the beginning of the desorption kinetics by using the parameters of direct coupling (*Fig. 14*). The diffusion coefficient D_{short} is multiplied by a factor of two. The diffuso-elastic coupling modifies the diffusion coefficient. So, even if this coupling does not model correctly the kinetics desorption, it must be taken into account in order to characterize the diffusion coefficient of CO_2 in PVF_2.

3.3 Direct Couplings and Indirect Couplings Comparison

The discussion compares the identical parameters of the direct couplings as defined in Figure 12. An indirect coupling is incorporated into the diffusion coefficient law Equation (5) by taking $D_0 = 1.5 \times 10^{-12}$ m^2.s^{-1} and the law Equation (22) for the β parameter. The diffuso-elastic coupling becomes negligible compared to the influence of the gas concentration. At the end of gas sorption, concentration in the material is high, inducing a high diffusion coefficient ($D_0 = 3.0 \times 10^{-12}$ m^2.s^{-1}) due to the law describing the dependency on

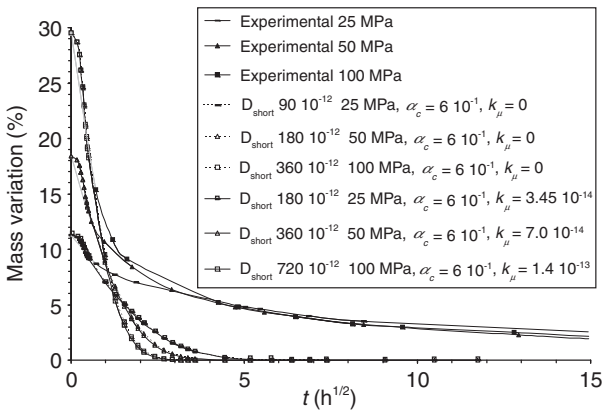

Figure 14

Desorption kinetics of CO_2, for high-pressure tests (25, 50 and 100 MPa), with constant D_{short} (Fick's law) multiplied by a factor at each level of pressure and a diffuso-elastic coupling.

concentration. So, at the beginning of the decompression the first term of Equation (12) is prevailing compared to the diffuso-elastic coupling, the second term of Equation (12).

So, when investigating the behavior of PVF_2 subjected to a CO_2 pressure fluctuation, it is necessary to simultaneously consider the direct and indirect couplings. The phenomenological laws, where D is a function of pressure and concentration, can describe the non linear behavior of CO_2 diffusion in PVF_2. However, the same laws are unable to describe the mechanical behavior of PVF_2 during the sorption-desorption of CO_2 in the material. Concerning the direct couplings, they can predict the change in volume of the material and the kinetics of diffusion. Nevertheless, as soon as the influence of pressure and concentration becomes important, the introduction of the indirect couplings into the direct couplings proves to be necessary in order to correctly describe the diffusion stage.

CONCLUSIONS

The present study brings out some pertinent conclusions about the type of diffuso-elastic couplings, that must be considered in order to describe the behavior of PVF_2 subjected to a CO_2 pressure fluctuation.

The diffusion coefficient becomes pressure and gas concentration dependent for pressures higher than 0.5 MPa. For the studied system, the effect of the pressure on the diffusion coefficient is relatively weak compared to that of the gas concentration. The β parameter related to gas/polymer interactions is a function of pressure. The prediction of desorption kinetics is as better as the degree of the dependency on concentration is high. Nevertheless for tests investigated at high pressures ($\geq$ 25 MPa), the phenomenological laws, for which D is a function of pressure and gas concentration, are insufficient to completely describe the desorption kinetics.

The direct diffuso-mechanical couplings from Rambert *et al.* [5, 32–34] give the volume strain threshold of PVF_2 at the end of the CO_2 sorption with an expansion coefficient connected to mass transport. This expansion coefficient is independent of the applied pressure. In this model, the coupling with the gradient of the volume strain introduced into the diffusion equation is insufficient to account for the highly non-linear behavior of the diffusion kinetics (high pressures $\geq$ 25 MPa). This coupling can be neglected compared to the effect of concentration on the diffusion coefficient during a solubility test.

In order to simultaneously describe the volume change of PVF_2 and the diffusion kinetics of CO_2 in PVF_2, it is necessary to consider concomitantly the indirect couplings and the direct couplings.

For high CO_2 pressure, desorption in PVF_2 usually takes place in a rubbery state and lasts several hundred hours. It would be relevant in the future to consider a diffuso-visco-elastic coupling rather than a diffuso-elastic one. Moreover, in order to take into account the residual mass and volume strain in the material, it appears necessary to develop a coupled model involving damage.

ACKNOWLEDGMENTS

This research started by a project in polymer 'blistering' completed in co-operation with IFP Energies nouvelles, Rueil-Malmaison, France [5, 6].

REFERENCES

1 Klopffer M.H., Flaconnèche B. (2001) Transport properties of gases in polymers: Bibliographic review, *Oil & Gas Science and Technology* **56**, 3, 223-244. DOI: 10.2516/ogst:2001021.

2 Benjelloun-Dabaghi Z., Benali A. (2001) Mathematical modelling of the permeation of gases in polymers, *Oil & Gas Science and Technology* **56**, 3, 295-303. DOI: 10.2516/ogst:2001025.

3 Benjelloun-Dabaghi Z., de Hemptinne J.C., Jarrin J., Leroy J.M., Aubry J.C., Saas J.N., Taravel-Condat C. (2002) MOLDI^{TM}: A fluid permeation model to calculate the annulus composition in flexible pipes, *Oil & Gas Science and Technology* **57**, 2, 177-192. DOI: 10.2516/ogst:2002014.

4 Jarrin J., Dewimille B., Devaux E., Martin J., Piques R. (1994) Blistering of thermoplastic materials used in the petroleum industry, *Society of Petroleum Engineers* **28482**, 203-214. DOI: 10.2118/28482-MS.

5 Rambert G., Grandidier J.C., Cangémi L., Meimon Y. (2003) A modelling of the coupled thermo-diffuso-elastic linear behaviour. Application to explosive decompression of polymers, *Oil & Gas Science and Technology* **58**, 5, 571-591. DOI: 10.2516/ogst:2003040.

6 Boyer S.A.E., Klopffer M.H., Martin J., Grolier J.E. (2007) Supercritical gas-polymer interactions with applications in the petroleum industry. Determination of thermophysical properties, *Journal of Applied Polymer Science* **103**, 3, 1706-1722. DOI: 10.1002/app. 25085.

7 Frisch H.L. (1957) The time lag in diffusion, *The Journal of Physical Chemistry* **61**, 1, 93-95. DOI: 10.1021/j150547a018.

8 Crank J., Park G.S. (1968) *Diffusion in polymers*, Academic Press, London and New-York.

9 Frisch H.L. (1970) Pressure dependence of diffusion in polymers, *Journal of Elastomers & Plastics* **2**, 2, 130-132. DOI: 10.1177/009524437000200206.

10 Fick A. (1995) On liquid diffusion, *Journal of Membrane Science* **100**, 1, 33-38. DOI: 10.1016/0376-7388(94)00230-V.

11 Prager S., Long F.A. (1951) Diffusion of hydrocarbons in polyisobutylene, *Journal of American Chemical Society* **73**, 9, 4072-4075. DOI: 10.1021/ja01153a004.

12 Crank J. (1953) A theoretical investigation of the influence of molecular relaxation and internal stress on diffusion in polymers, *Journal of Polymer Science* **11**, 2, 151-168. DOI: 10.1002/pol.1953.120110206.

13 Barrer R.M. (1957) Some properties of diffusion coefficients in polymers, *The Journal of Physical Chemistry* **61**, 2, 178-189. DOI: 10.1021/j150548a012.

14 Frisch H.L. (1980) Sorption and transport in glassy polymers - A review, *Polymer Engineering and Science* **20**, 1, 2-13. DOI: 10.1002/pen.760200103.

15 Benjelloun-Dabaghi Z. (2001) Analyse de quelques modèles de diffusion 1D non linéaire des gaz dans les polymères : identification à partir des données expérimentales, *Oil & Gas Science and Technology* **56**, 3, 279-293. DOI: 10.2516/ogst:2001024.

16 Suwandi M.S., Stern S.A. (1973) Transport of heavy organic vapors through silicone rubber, *Journal of Polymer Science: Polymer Physics Edition* **11**, 4, 663-681. DOI: 10.1002/pol.1973.180110404.

17 Rogers C.E. (1985) Permeation of Gases and Vapours in Polymers, in *Polymer Permeability*, Comyn J. (ed.), Chapman & Hall, pp. 11-73. DOI: 10.1007/978-94-009-4858-7_2.

18 Naito Y., Kamiya Y., Terada K., Mizoguchi K., Wang J.S. (1996) Pressure dependence of gas permeability in a rubbery polymer, *Journal of Applied Polymer Science* **61**, 6, 945-950. DOI: 10.1002/(SICI)1097-4628(19960808)61:6<945::AID-APP8>3.0.CO;2-H.

19 Fujita H., Kishimoto A., Matsumoto K. (1960) Concentration and temperature dependence of diffusion coefficients for systems polymethyl acrylate and *n*-alkyl acetates, *Transactions of the Faraday Society* **56**, 424-437. DOI: 10.1039/TF9605600424.

20 Stern S.A., Fang S.M., Frisch H.L. (1972) Effect of pressure on gas permeability coefficients. A new application of "free volume" theory, *Journal of Polymer Science Part A-2: Polymer Physics* **10**, 2, 201-219. DOI: 10.1002/pol.1972.160100202.

21 Stern S.A., Fang S.M., Frisch H.L. (1972) Effect of pressure on gas permeability coefficients. A new application of "free volume" theory, *Journal of Polymer Science Part A-2: Polymer Physics* **10**, 3, 575. DOI: 10.1002/pol.1972.160100315.

22 Naito Y., Mizoguchi K., Terada K., Kamiya Y. (1991) The effect of pressure on gas permeation through semicrystalline polymers above the glass transition temperature, *Journal of Polymer Science Part B: Polymer Physics* **29**, 4, 457-462. DOI: 10.1002/polb.1991.090290408.

23 Naito Y., Bourbon D., Terada K., Kamiya Y. (1993) Permeation of high-pressure gases in poly(ethylene-co-vinylacetate), *Journal of Polymer Science Part B: Polymer Physics* **31**, 6, 693-697. DOI: 10.1002/polb.1993.090310609.

24 Benali A., Benjelloun-Dabaghi Z., Flaconnèche B., Klopffer M.H., Martin J. (2001) Analyse et simulation de l'influence de la température et de la pression sur les coefficients de transport du CO_2 dans du PVDF, *Oil & Gas Science and Technology* **56**, 3, 305-312. DOI: 10.2516/ogst:2001026.

25 Petropoulos J.H. (1984) Sorption-longitudinal swelling kinetic correlations in polymer film-vapor systems, *Journal of Membrane Science* **17**, 3, 233-244. DOI: 10.1016/S0376-7388(00)83215-9.

26 Govindjee S., Simo J.C. (1993) Coupled stress diffusion: case II, *Journal of the Mechanics and Physics of Solids* **41**, 5, 863-887. DOI: 10.1016/0022-5096(93)90003-X.

27 Shanati S., Ellis N.S., Randall T.J., Marshall J.M. (1995) Coupled diffusion and stress by the finite element method, *Applied Mathematical Modelling* **19**, 2, 87-94. DOI: 10.1016/0307-904X(94)00019-3.

28 Jou D., Casas-Vazquez J., Lebon G. (2001) Non classical diffusion, in *Extended irreversible thermodynamics, 3rd Edition*, Jou D., Casas-Vazquez J., Lebon G. (eds.), Springer, pp. 295-314. DOI: 10.1007/978-3-642-56565-6.

29 Hansen H. (2004) Aspects of solubility, surfaces and diffusion in polymers, *Progress in Organic Coatings* **51**, 1, 55-66. DOI: 10.1016/j.porgcoat.2004.05.002.

30 Piccinini E., Gardini D., Doghieri F. (2006) Stress effects on mass transport in polymers: a model for volume relaxation, *Composites Part A: Applied Science and Manufacturing* **37**, 4, 546-555. DOI: 10.1016/j.compositesa.2005.05. 001.

31 Minelli M., Sarti G.C. (2013) Permeability and diffusivity of CO_2 in glassy polymers with and without plasticization, *Journal of Membrane Science* **435**, 176-185. DOI: 10.1016/j.memsci.2013.02.013.

32 Rambert G., Grandidier J.C. (2005) An approach to the coupled behaviour of polymers subjected to a thermo-mechanical loading in a gaseous environment, *European Journal of Mechanics - A/Solids* **24**, 1, 151-168. DOI: 10.1016/j.euromechsol.2004.10.005.

33 Rambert G., Jugla G., Grandidier J.C., Cangemi L. (2006) A modelling of the direct couplings between heat transfer, mass transport, chemical reactions and mechanical behaviour. Numerical implementation to explosive decompression, *Composites: Part A Applied Science and Manufacturing* **37**, 4, 571-584. DOI: 10.1016/j.compositesa.2005.05.021.

34 Rambert G., Grandidier J.C., Aifantis E.C. (2007) On the direct interactions between heat transfer, mass transport and chemical processes within gradient elasticity, *European Journal of Mechanics - A/Solids* **26**, 1, 68-87. DOI: 10.1016/j.euromechsol.2005.12.002.

35 Baudet C., Grandidier J.C., Cangémi L., Klopffer M.H. (2006) Numerical modeling of the PVF_2 volume strain with carbone dioxide, *Oil & Gas Science and Technology* **61**, 6, 751-757. DOI: 10.2516/ogst:2006013.

36 Baudet C., Grandidier J.C., Cangémi L. (2009) A two-phase model for the diffuso-mechanical behaviour of semi-crystalline polymers in gaseous environment, *International Journal of Solids and Structures* **46**, 6, 1389-1401. DOI: 10.1016/j.ijsolstr.2008.11.010.

37 Baudet C., Grandidier J.C., Cangémi L. (2011) A damage model for the blistering of polyvinylidene fluoride subjected to carbon dioxide decompression, *Journal of the Mechanics and Physics of Solids* **59**, 9, 1909-1926. DOI: 10.1016/j.jmps.2011.04.010.

38 Flaconnèche B., Martin J., Klopffer M.H. (2001) Permeability, diffusion and solubility of gases in polyethylene, polyamide 11 and poly(vinylidene fluoride), *Oil & Gas Science and Technology* **56**, 3, 261-278. DOI: 10.2516/ogst:2001023.

39 Bazourdy E., Martin J. (1999) IFP Energies nouvelles report.

40 Flaconnèche B., Martin J., Klopffer M.H. (2001) Transport properties of gases in polymers: experimental methods, *Oil & Gas Science and Technology* **56**, 3, 245-259. DOI: 10.2516/ogst:2001022.

41 Rogers C.E. (1964) Permeability and chemical resistance, in *Engineering Design for Plastics*, Baer E. (ed.), Reinhold, New York, pp. 609-688.

42 Comyn J. (1985) *Polymer permeability*, Comyn J. (ed.), Elsevier Applied Science Publishers, London/New York.

43 Neogi P. (1996) *Diffusion in Polymers*, Neogi P. (ed.), Marcel Dekker, New York, p. 173.

44 Stancel A.F. (1971) *Diffusion through polymers*, Tobolsky A.V., Mark H.F. (eds.), Polymer Science and Materials, p. 247.

45 Naylor T.V. (1989) Permeation properties, in *Comprehensive Polymers Science*, Booth C., Price C. (eds.), Pergamon Press, Oxford, **2**, 643-668.

Manuscript accepted in October 2013
Published online in May 2014

Cite this article as: J.-C. Grandidier, C. Baudet, S.A.E. Boyer, M.-H. Klopffer and L. Cangémi (2015). Diffuso-Kinetics and Diffuso-Mechanics of Carbon Dioxide / Polyvinylidene Fluoride System under Explosive Gas Decompression: Identification of Key Diffuso-Elastic Couplings by Numerical and Experimental Confrontation, *Oil Gas Sci. Technol* **70**, 2, 251-266.